[Article ID] 1003- 6326(2001)01- 0022- 04

Stress corrosion cracking of brass in ammonia solution①

GUO Xian-zhong(郭献忠), GAO Ke-wei(高克玮), QIAO Li-jie(乔利杰), CHU Wu-yang(褚武扬)
(Department of Materials Physics, University of Science and Technology Beijing, Beijing 100083, P. R. China)

[Abstract] Brass foil with a protective layer formed on one side was deflected during corrosion in an ammonia solution under various applied potentials, and then corrosion-induced stress generated at brass/dezincification layer under different potentials could be measured. At the same time, susceptibility to stress corrosion cracking(SCC) of brass in the ammonia solution under various applied potentials was measured using a single-edge notched specimen. At open-circuit potential, both corrosion-induced tensile stress and susceptibility to SCC(I_0) had a maximum value. Both tensile stress σ_p and susceptibility I_0 decreased slightly under anodic polarization, but reduced steeply with the decrease in potential of cathodic polarization. At the cathodic potential of - 500 mV(vs SCE), corrosion-induced stress became compressive because of copper-plating layer, correspondingly, susceptibility to SCC was zero. Therefore, the variation of SCC susceptibility with potential is consistent with that of the corrosion-induced additive stress.

[Key words] brass; corrosion-induced stress; stress corrosion cracking
[CLC number] TG172.9; TG146.1 [Document code] A

1 INTRODUCTION

The TEM observations showed[1~4] that the corrosion process itself can facilitate dislocation emission and motion during stress corrosion cracking(SCC) of brass, 310 stainless steel, and Ti_3Al+ Nb. Nano-crack of SCC will nucleate in a dislocation free zone (DFZ) only when the corrosion-enhanced dislocation emission and motion develop into a critical condition. It has been proposed that vacancies induced by anodic dissolution can facilitate the climb of edge dislocation, which results in anodic polarization-enhanced ambient creep[5,6]. The TEM observations, however, showed that corrosion process during SCC enhances dislocation emission, multiplication and motion and these dislocations tend to glide over slip planes instead of climb[1~4]. So, there must exist another mechanism for the corrosion-enhanced dislocation emission and motion in addition to the divacancy-enhanced dislocation climb.

Many experiments showed that large tensile or compressive stress would generate at the interface between metal and passive film during anodic polarization in a solution using a potentiostat[7]. Numerous stress-generating mechanisms have been proposed[7], for example, such induced tensile has been reported during the anodic polarization of α-Ti in 0.1 mol/L H_2SO_4 solution[7], in which no SCC occurs. During original corrosion for the α-Ti in the same solution, the additive tensile stress grows gradually, and reaches a maximum value of 313 MPa, which approaches the yield stress of α-Ti[8].

The brass foil with a protective layer formed on one side was deflected during original corrosion in 1 mol/L NH_4OH+ 5 g/L $CuCl_2$ solution[9]. This is due to corrosion-induced tensile stress developed at the interface between metal and dezincification layer, which grew gradually, and reached a steady value[9].

Stress corrosion cracking (SCC) for brass in the ammonia solution is controlled by anodic dissolution, and a dezincification layer forms during SCC. The corrosion-induced tensile stress generated at the metal/dezincification layer interface exists also during SCC, and has the same orientation with an applied stress. Therefore, the corrosion-induced stress possibly assists the applied stress to prompt SCC. If so, there is certainly a relationship between susceptibility to SCC and the corrosion-induced stress. Susceptibility to SCC of brass in the ammonia solution strongly depends upon applied potential[10]. Therefore, in this paper, we will simultaneously measure corrosion-induced tensile stress generated at the metal/dezincification layer and susceptibility to SCC for brass in the ammonia solution under various applied potentials, and then look for the relationship between the corrosion-induced stress and SCC susceptibility.

2 EXPERIMENTAL

The material used is brass with 38% Zn and has the yield strength of 131 MPa. The foil specimens with dimensions of 0.2 mm × 5 mm × 90 mm were polished down to 1000 grit finish, and then annealed in vacuum at 280 ℃ for 1.5 h. Measuring deflection

① [Foundation item] Project (G19990650) supported by the Special Funds for the Major State Basic Research Projects and projects (50071010; 19891180) supported by the National Natural Science Foundation of China [Received date] 2000- 03- 15; [Accepted date] 2000- 07- 24

during the original corrosion process was performed by the Stoney method[7,8] and the detail was shown in Refs. [8, 9]. The calibration showed that $\delta/L = 0.362x/D$[9], where δ is the deflection, L (= 60 mm) the length of the specimen immersed in the solution, D (= 1 000 mm) the distance between a mirror attached to the free end of the specimen and telescope, x the reading of ruler telescope. Measuring $x(t)$ during corrosion process under various potentials, $\delta(t) = 2.1 \times 10^{-2} x(t)$ was obtained. During original corrosion in 1 mol/L NH_4OH + 5 g/L $CuCl_2$ solution, potential varied from − 395 mV to − 420 mV. Applied constant potentials were − 350 mV, − 400 mV (anodic polarization), and − 420 mV, − 440 mV, − 460 mV and − 500 mV (cathodic polarization), respectively.

In order to determine the thickness of dezincification layer d, one side of the sample and half part of the other side are coated with a 1720 enamel and immersed in the ammonia solution under various potentials. The average thickness of the dezincification layer after corrosion for different times was measured in SEM with the coated part of the sample as a reference.

The single-edge notched specimens with dimensions of 0.2 mm × 10 mm × 95 mm, containing a notch of 5 mm depth and root radius of 0.1 mm, were extended at a rate of 1.89×10^{-5} mm/s in air and the ammonia solution under various potentials, respectively. Susceptibility to SCC was evaluated in term of $I_t = (1 - t_{F,sol}/t_{F,air}) \times 100\%$ or $I_\sigma = (1 - \sigma_{F,sol}/\sigma_{F,air}) \times 100\%$, where $t_{F,air}$, $\sigma_{F,air}$ and $t_{F,sol}$, $\sigma_{F,sol}$ are the fracture time and the nominal fracture stress during the slow extension in air and the solution, respectively.

3 EXPERIMENTAL RESULTS

Deflection δ vs corrosion time at open-circuit potential for five specimens is plotted in Fig. 1(a). As the active surface of the foil specimen becomes concave during original corrosion, a tensile stress is generated at the brass/dezincification layer interface[8]. Deflection vs corrosion time under various potentials is plotted in Fig. 1(b), which shows that anodic polarization, i. e. applied potential of − 350 mV and − 420 mV, increases the deflection, while cathodic polarization decreases the deflection. The specimen was copper-plating at cathodic polarization of − 500 mV, and the active surface became convex in stead of concave, resulting in a compressive stress generated at the brass/copper-plating layer interface.

The thickness of dezincification layer increases linearly with increasing corrosion time at open-circuit potential, as shown in Fig. 2.

The deflections after corrosion under various potentials for 40 min are listed in Table 1. The average thickness of the dezincification layer after corrosion under various potentials for 40 min is also listed in Table 1. The stress generated at the brass/dezincification layer interface can be calculated based on equation[8,9] $\sigma_p = Eh^2\delta/[3(1-\upsilon^2)L^2d]$, where E and υ are the elastic modulus and Poisson's ratio of

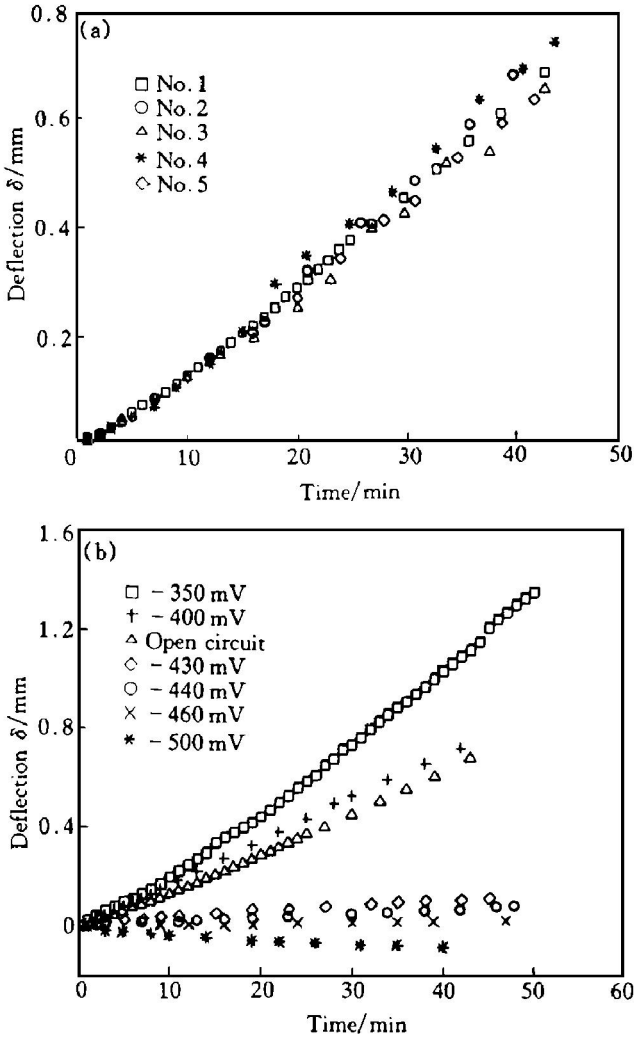

Fig. 1 Deflection vs corrosion time at original corrosion (a) and under various potentials (b)

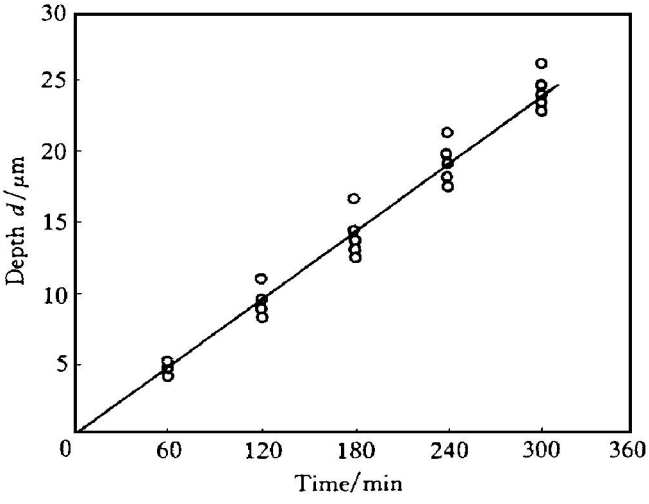

Fig. 2 Depth of dezincification layer vs time under original corrosion potential

metal strip of length, L, and thickness, h. The stress σ_p is an average stress of whole specimen, and are also listed in Table 1. The results extended in air and in the ammonia solution under various potentials are listed in Table 2, where I_t and I_σ are susceptibility to SCC.

Table 1 Deflection δ, thickness of dezincification layer d and stress under various potentials

V/mV	δ/mm	d/μm	σ_p/MPa
- 350	1.01, 1.03	5.32	84.8, 86.5
- 400	0.67, 0.69	3.81	78.6, 80.9
- 410*	0.59, 0.61, 0.62, 0.62, 0.67	3.18	82.9, 85.7, 87.1, 87.1, 94.1
- 430	0.11	0.73	67.3
- 440	0.05, 0.06	0.51	43.8, 52.6
- 460	0.01	0.10	44.7
- 500	- 0.08	3.0	- 11.9

* Open-circuit potential

Table 2 Fracture time t_F, nominal fracture stress σ_F and SCC susceptibility under various potentials

V/mV	t_F/h	σ_F/MPa	I_t/%	I_σ/%
Air	37, 39, 41	203, 217, 230	-	-
- 350	4, 4.2	51, 51	90, 89	77
- 400	4.7, 5	56, 56	88, 87	74
- 410*	3, 4	39, 40	92, 90	82, 81
- 420	5	56	87	74
- 430	5.5	67	86	69
- 440	10, 11	73, 79	74, 72	66, 64
- 446	14	118	64	46
- 460	38	180	0	17
- 500	34	214	0	0

* Open-circuit potential

The variation of SCC susceptibility with potential is consistent with that of the corrosion-induced stress, as shown in Fig. 3. Fig. 3 shows that both

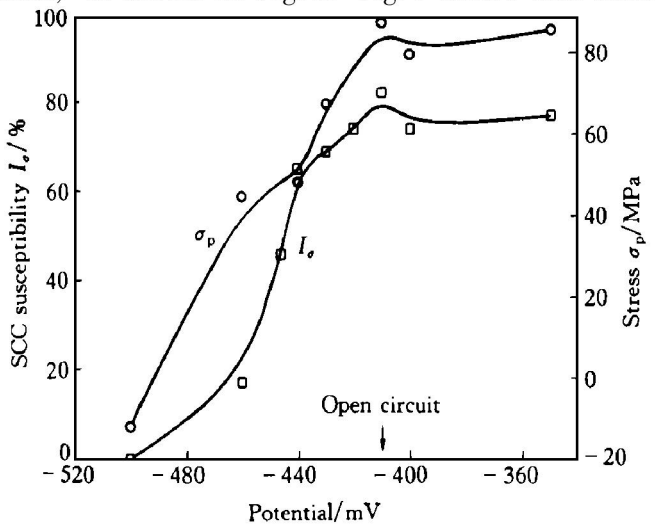

Fig. 3 Susceptibility to SCC and corrosion-induced stress vs potential

SCC susceptibility and the corrosion-induced stress decrease slightly under anodic polarization, but reduce steeply with the decrease in cathodic polarization. When applied potential is less than - 460 mV, the corrosion-induced stress is zero or compressive, and then no SCC occurs.

4 DISCUSSION

There is a considerable amount of vacancies and voids in the dezincification layer because of the selective dissolution of Zn. The vacancies and voids will make the porous dezincification layer near the surface shrink, the other part of the specimen, however, will hinder the shrinkage of the dezincification layer, resulting in a tensile stress generated at the interface of the metal/dezincification layer. Kevin et al[11] calculated stress distribution of Au-Cu alloy with de-alloying porous layer through the methods of continuum eigenstrain analysis. The result indicated that a tensile stress of 70 MPa generated at the interface of the alloy/porous layer. The stress listed in Table 1 is an average over the thickness of the specimen, which is much less than that generated at the interface of the metal/dezincification layer.

The corrosion-induced tensile stress σ_p exists also during SCC in the same solution, and has the same orientation with an applied stress σ_a. Therefore, the stress intensity factor for the single-edge notched specimen during SCC is $K_I(\mathrm{SCC}) = 1.12(\sigma_a + \sigma_p)\sqrt{\pi a} = K_{Ia} + K_{Ip}$, where K_{Ia} is an applied stress intensity factor, and K_{Ip} an additive stress intensity factor resulting from corrosion-induced tensile stress. When $K_I(\mathrm{SCC})$ increases to a critical value of K_{IC}, the specimen fails during SCC. Hence, the critical applied stress intensity factor necessary for SCC will be $K_{IC} - K_{Ia}$, which is less than K_{IC}. That is to say that the corrosion-induced tensile stress will assist the applied stress to facilitate SCC. Fig. 3 shows that if there is no corrosion-induced tensile stress, no SCC occurs, and susceptibility to SCC is consistent with the corrosion-induced stress. Therefore, the corrosion-induced tensile stress plays an important part in SCC.

5 CONCLUSIONS

1) A tensile stress will be generated at the metal/dezincification layer interface during original corrosion for brass in an ammonia solution. The corrosion-induced stress decreases slightly under anodic polarization, but reduces steeply with the decrease in cathodic polarization, and becomes compressive at the potential of - 500 mV.

2) The variation of SCC susceptibility with applied potential is consistent with that of the corrosion-induced stress.

[REFERENCES]

[1] GU B, ZHANG J W, WANG F R, et al. The in-situ TEM observation of corrosion facilitating dislocation emission, multiplication and motion for brass [J]. Scripta Metall, 1995, 32(4): 637- 640.

[2] CHU W Y, GU B, GAO K W, et al. Corrosion-enhanced dislocation emission and motion resulting in initiation of stress corrosion cracking [J]. Science in China, 1997, 40(3): 235- 242.

[3] GAO K W, WANG Y B, CHU W Y, et al. In-situ TEM observation of dissolution-enhanced dislocation emission, motion and the nucleation of SCC for Ti-24Al-11Nb alloy in methanol [J]. Scripta Metall, 1997, 36(2): 259- 264.

[4] HUANG Y Z, CHEN Q Z and CHU W Y. In-situ TEM observation of dislocation emission and motion induced by anodic dissolution in type 310 stainless steel [J]. J Mater Sci Tech, 1996, 12(3): 215- 218.

[5] Uhlig H H. Effect of surface dissolution on plastic deformation of iron and steel [J]. J Electrochem Soc, 1976, 123(11): 1699- 1701.

[6] GU B, CHU W Y, CHU W, et al. The effect of anodic polarization on the ambient creep of brass [J]. Corrosion Sci, 1994, 36(8): 1437- 1445.

[7] Nelson J C and Oriani R A. Stress generation during anodic oxidation of titanium and aluminum [J]. Corrosion Sci, 1993, 34(2): 307- 326.

[8] LU H, GAO K W and CHU W Y. Determination of tensile stress induced by oxide film during corrosion process for α-Ti [J]. Scripta Metall, 1997, 37(9): 1387- 1391.

[9] LU H, GAO K W and CHU W Y. Investigation of tensile stress induced by dezincification layer during corrosion for brass [J]. Corrosion Sci, 1998, 40(10): 1663- 1670.

[10] Jones R H. Stress-Corrosion Cracking [M]. ASM Inter Materials Park, 1992. 211- 231.

[11] Kevin M and Ferrar M. On corrosion-induced stress states in binary noble metal alloys [J]. Mater Sci Eng, 1997, A232(7): 88- 102.

(Edited by PENG Chao-qun)